Supplement of Earth Syst. Dynam., 10, 631–650, 2019
https://doi.org/10.5194/esd-10-631-2019-supplement

Earth System Dynamics
Open Access
EGU

Supplement of

Tipping the ENSO into a permanent El Niño can trigger state transitions in global terrestrial ecosystems

Mateo Duque-Villegas et al.

Correspondence to: Juan Fernando Salazar (juan.salazar@udea.edu.co)

Supplementary information

List of Tables

List of Figures

Table S1. Observational data sets derived from satellite and ground-based measurements.

Quantity	Data set	Institution	Period	Grid res.	Step	Reference
Surface temperature ($^\circ$C)	AMIP II v.1.1.3	PCMDI	1979–2010	1°	Monthly	Hurrell et al. (2008)
Near surface temperature ($^\circ$C)	HadCRUT4 v.4.6.0	Met Office Hadley Centre, Climatic Research Unit, University of East Anglia	1988–2017	5°	Monthly	Morice et al. (2012)
Precipitation ($\mathrm{mm\,day^{-1}}$)	GPCP v.2.3	WCRP/GEWEX	1987–2016	2.5°	Monthly	Adler et al. (2003)
Mean sea-level pressure (mb)	HadSLP2	Met Office Hadley Centre	1979–2004	5°	Monthly	Allan and Ansell (2006)
GPP ($\mathrm{dg\,C\,m^{-2}\,year^{-1}}$)	MOD17A2 v.55	Numerical Terradynamic Simulation Group, University of Montana	2000–2015	1 km	Monthly	Zhao et al. (2005)
Surface temperature (K)	PRISM3 v.1.0	U.S. Geological Survey	Climatology	$1^\circ \times 2^\circ$	Monthly	Dowsett et al. (2009)

Table S2. Data obtained from ERA-Interim reanalysis (Dee et al., 2011). All data had a 2.5° horizontal resolution and covered the time span 1987–2016.

Quantity	Parameter	Stream	Time	Step
At pressure levels 50–1000 hPa:				
Air temperature (K)	130	MODA	–	–
Zonal wind ($\mathrm{m\,s^{-1}}$)	131	MODA	–	–
Meridional wind ($\mathrm{m\,s^{-1}}$)	132	MODA	–	–
Radiation budget:				
Surface sensible heat flux ($\mathrm{J\,m^{-2}}$)	146	MNTH	00:00,12:00	12
Surface latent heat flux ($\mathrm{J\,m^{-2}}$)	147	MNTH	00:00,12:00	12
Surface solar radiation downwards ($\mathrm{J\,m^{-2}}$)	169	MNTH	00:00,12:00	12
Surface thermal radiation downwards ($\mathrm{J\,m^{-2}}$)	175	MNTH	00:00,12:00	12
Surface net solar radiation ($\mathrm{J\,m^{-2}}$)	176	MNTH	00:00,12:00	12
Surface net thermal radiation ($\mathrm{J\,m^{-2}}$)	177	MNTH	00:00,12:00	12
Top net solar radiation ($\mathrm{J\,m^{-2}}$)	178	MNTH	00:00,12:00	12
Top net thermal radiation ($\mathrm{J\,m^{-2}}$)	179	MNTH	00:00,12:00	12
Total incoming solar radiation ($\mathrm{J\,m^{-2}}$)	212	MNTH	00:00,12:00	12
Water budget:				
Evaporation (m)	182	OPER	00:00,12:00	12
Total precipitation (m)	228	OPER	00:00,12:00	12
Total column water vapour (mm)	137	MODA	–	–
For meridional stream function:				
Surface pressure (Pa)	134	MODA	–	–

Table S3. Global averages for annual mean and seasonal means from observational data sets and experiments CTL, PEN, as well as the p-value of the hypothesis that both experiments have the same sample mean ($\alpha = 0.05$). Two asterisks (**) are used when the p-value is below 10^{-5}. Results for land-only and ocean-only fields are shown too.

Variable	**Data**	**Annual**			**DJF**			**MAM**			**JJA**			**SON**		
		Global	*Land*	*Ocean*	*Global*	*Land*	*Ocean*	*Global*	*Land*	*Ocean*	*Global*	*Land*	*Ocean*	*Global*	*Land*	*Ocean*
Near surface temperature ($^\circ$C)	HadCRUT4	14.3	13.4	15.5	12.6	11.0	14.8	14.3	13.4	15.2	16.1	15.4	16.3	14.4	13.7	15.7
	CTL	13.9	14.3	14.1	11.7	11.1	13.2	13.4	13.7	13.7	15.9	17.1	15.0	14.4	15.3	14.6
	PEN	14.4	15.1	14.6	12.4	12.2	13.7	14.0	14.6	14.1	16.3	17.8	15.3	14.9	15.9	15.2
	p-value	**	**	**	**	**	**	**	**	**	**	**	**	**	**	**
Precipitation ($\mathrm{mm\,day^{-1}}$)	GPCP	2.7	2.3	2.9	2.7	2.4	2.3	2.7	2.3	2.8	2.7	2.4	2.8	2.7	2.2	3.0
	CTL	2.8	2.6	3.0	2.8	2.8	3.0	2.9	2.5	3.0	2.9	2.5	2.9	2.7	2.7	2.9
	PEN	2.9	2.5	3.0	2.8	2.6	3.1	2.9	2.4	3.1	2.9	2.3	3.0	2.8	2.6	2.9
	p-value	**	**	**	**	**	**	**	**	**	0.0732	**	**	**	**	**
GPP ($\mathrm{kg\,C\,m^{-2}\,year^{-1}}$)	MODIS	0.2	0.8	–	0.2	0.8	–	0.2	0.8	–	0.3	0.9	–	0.2	0.8	–
	CTL	0.2	0.7	–	0.1	0.7	–	0.2	0.7	–	0.2	0.7	–	0.2	0.7	–
	PEN	0.2	0.6	–	0.1	0.6	–	0.2	0.6	–	0.2	0.7	–	0.1	0.6	–
	p-value	**	**	–	**	**	–	**	**	–	**	**	–	**	**	–
Mean sea-level pressure (hPa)	HadSLP2	1011.4	960.6	1007.8	1011.6	961.4	1007.0	1011.4	960.3	1008.0	1011.2	959.9	1008.6	1011.3	960.7	1007.6
	CTL	1012.0	961.0	1008.6	1012.3	962.3	1007.6	1012.1	961.2	1008.8	1011.6	960.0	1009.5	1011.9	960.7	1008.6
	PEN	1012.0	961.1	1008.6	1012.3	962.2	1007.6	1012.1	961.4	1008.7	1011.6	960.2	1009.5	1011.9	960.8	1008.5
	p-value	**	**	**	**	0.005	0.4261	**	**	**	**	**	**	**	**	**

Table S4. Energy budget values for CTL simulation and observations from ERA-Interim and Trenberth, Fasullo, and Mackaro (2011), as well as for PEN simulation and its difference with respect to CTL. The p-value is from the Student's t-test for experiments' sample means equality ($\alpha = 0.05$). Two asterisks (**) are used when the p-value is below 10^{-5}. Units are Wm^{-2}.

Variable	**CTL**	**ERA-Interim**	**TFM11**	**PEN**	**PEN − CTL**	**p-value**
TOA solar outgoing	108.8	100.2	101.9	108.4	−0.4	**
TOA solar incoming	341.3	344.2	341.3	341.3	0.0	0.994
TOA thermal outgoing	232.1	245.4	238.5	233.3	1.2	**
TOA net radiation	0.4	−1.4	0.9	−0.4	−0.8	**
Solar reflected atmosphere	83.0	76.4	78.8	82.7	−0.3	**
Solar absorbed atmosphere	68.7	80.1	78.0	69.1	0.4	**
Thermal emitted atmosphere	170.6	189.1	168.5	172.4	1.8	**
Solar reflected surface	25.8	23.8	23.1	25.7	−0.1	**
Solar absorbed surface	163.7	163.9	161.2	163.8	0.1	0.00023
Latent heat flux	82.0	83.8	80.0	83.0	1.0	**
Sensible heat flux	18.9	17.5	17.0	19.3	0.4	**
Thermal up surface	391.8	398.0	396.0	394.9	3.1	**
Thermal down surface	330.3	341.7	333.0	334.0	3.7	**

Table S5. Water budget values for CTL simulation and observations from ERA-Interim and Trenberth, Fasullo, and Mackaro (2011), as well as for PEN simulation and its difference with respect to CTL. The p-value is from the Student's t-test for experiments' sample means equality ($\alpha = 0.05$). Two asterisks (**) are used when the p-value is below 10^{-5}. Units are $1000\,\mathrm{km}^3\,\mathrm{year}^{-1}$.

Variable	**CTL**	**ERA-Interim**	**TFM11**	**PEN**	**PEN − CTL**	**p-value**
Land precipitation	125.4	114.5	114.0	121.3	−4.1	**
Land evapotranspiration	97.9	86.1	74.0	95.5	−2.4	**
Land net water flux	27.5	28.4	40.0	25.8	−1.7	**
Ocean precipitation	396.5	420.8	386.0	407.2	10.7	**
Ocean evaporation	424.0	447.3	426.0	432.9	8.9	**
Ocean net water flux	27.5	26.5	40.0	25.7	−1.8	**
Atmospheric water content	13.3	12.3	12.7	13.8	0.5	**

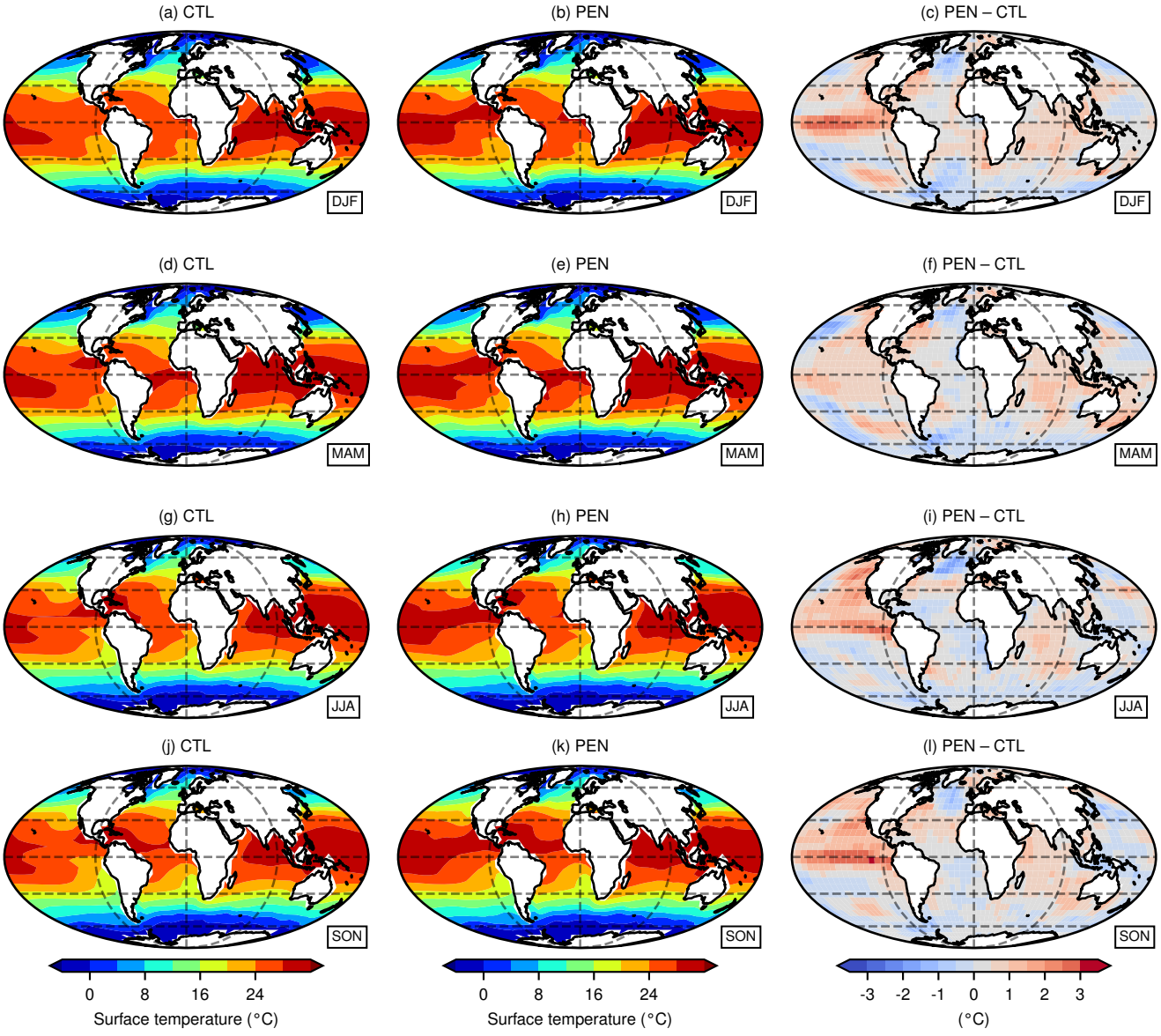

Figure S1. Prescribed SST climatology seasonal means for CTL (a, d, g, j) and PEN (b, e, h, k) simulations and their absolute differences (c, f, i, l). Grid lines are spaced every 30° from the Equator and 90° from Greenwich, in latitude and longitude respectively.

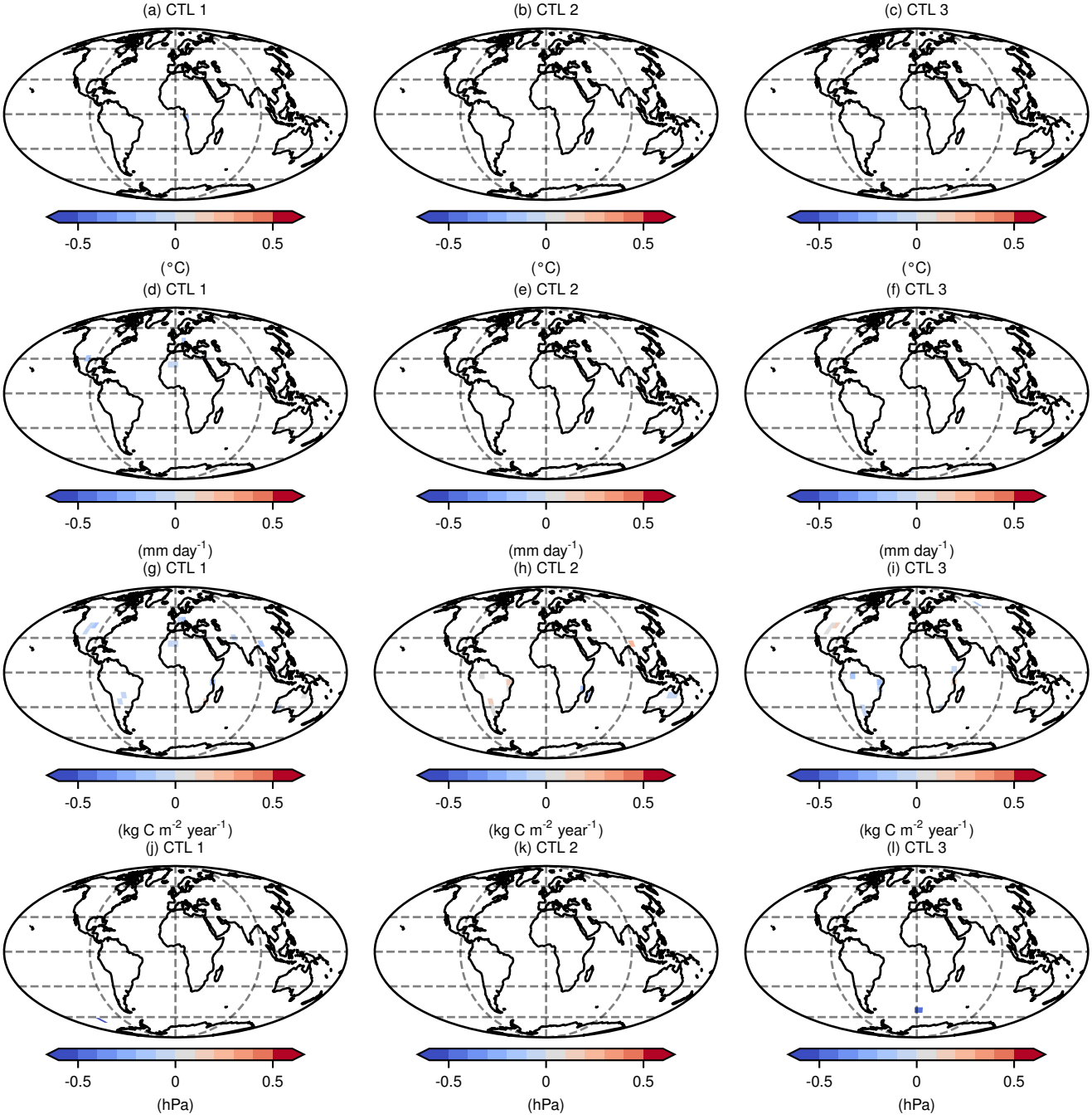

Figure S2. Annual mean differences of ensemble members versus the ensemble mean for CTL simulation for variables: near surface temperature (a, b, c), total precipitation rate (d, e, f), gross primary production (g, h, i) and mean sea-level surface pressure (j, k, l). In all panels white is for statistically non-significant differences ($\alpha = 0.05$). Grid lines are spaced every 30° from the Equator and 90° from Greenwich, in latitude and longitude respectively.

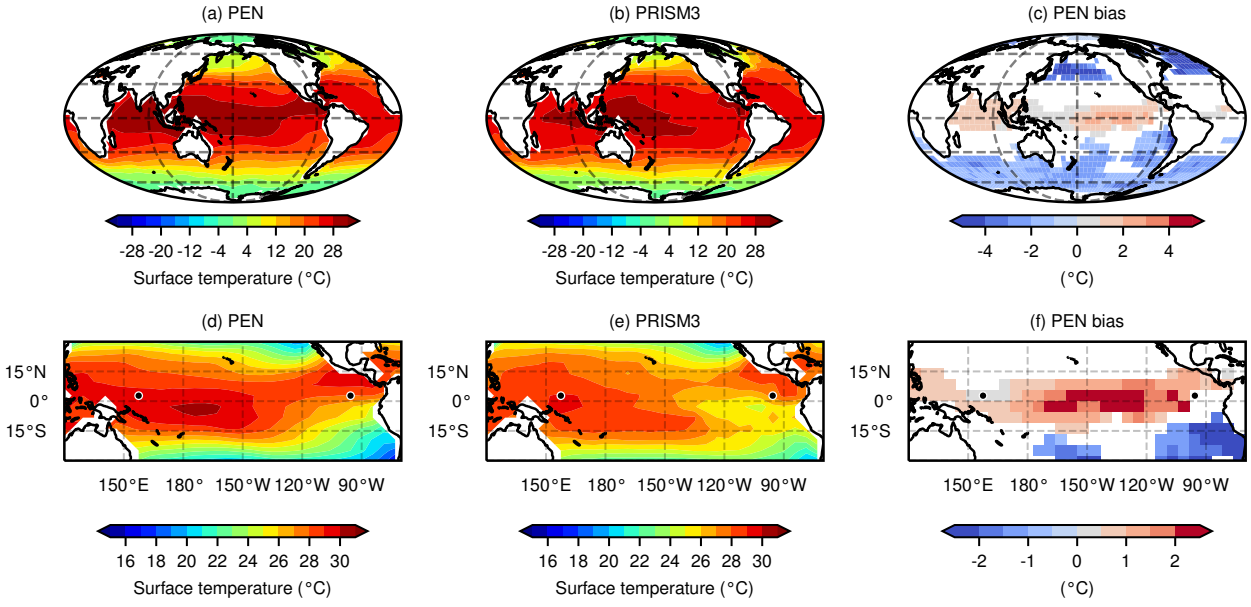

Figure S3. (top) Sea surface temperature forcing in PEN simulation (a), PRISM3 data set (b) and their differences (c). Grid lines are spaced every 30° from the Equator and 90° from Greenwich, in latitude and longitude respectively. (bottom) Equatorial Pacific sea surface temperature forcing in PEN simulation (d), PRISM3 data set (e) and their differences (f). Markers show the west (158° E, 2.8° N) and east (96° W, 2.8° N) sites used to compute the zonal gradient. In all bias panels white is for statistically non-significant differences ($\alpha = 0.05$).

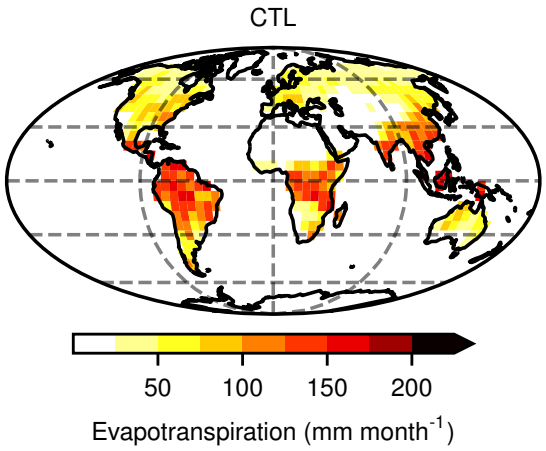

Figure S4. Annual mean evapotranspiration result for the CTL simulation used for calculating MCWD. Grid lines are spaced every 30° from the Equator and 90° from Greenwich, in latitude and longitude respectively.

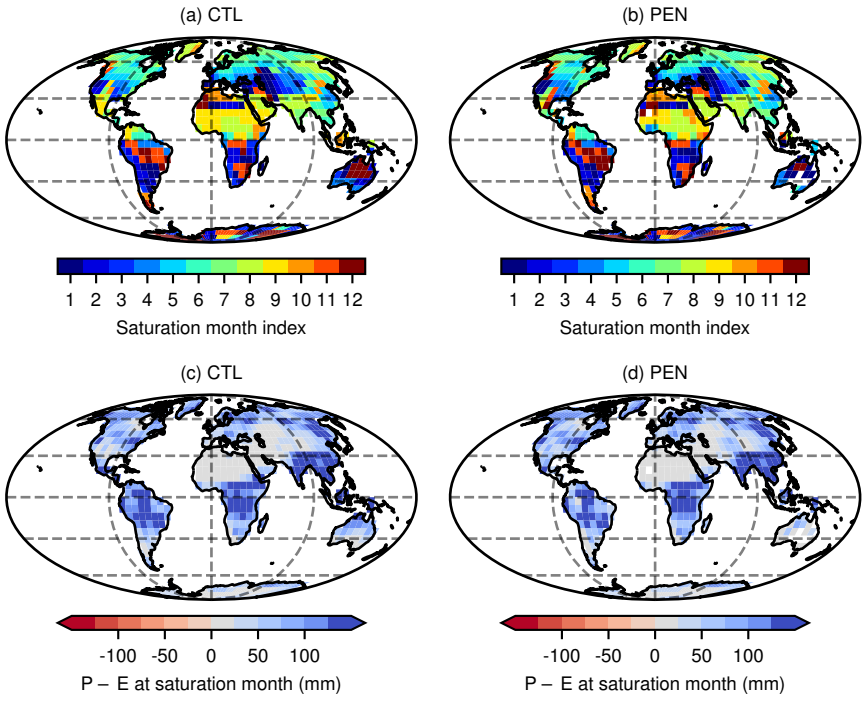

Figure S5. (top) Saturation month used in the calculation of MCWD for CTL (a) and PEN (b). The first month is January and the last month is December. (bottom) During these months precipitation (P) exceeded evapotranspiration (E) in each gridpoint, saturating ground conditions in CTL (c) and PEN (d). Water deficit accumulation is thus assumed to start at zero. Grid lines are spaced every 30° from the Equator and 90° from Greenwich, in latitude and longitude respectively.

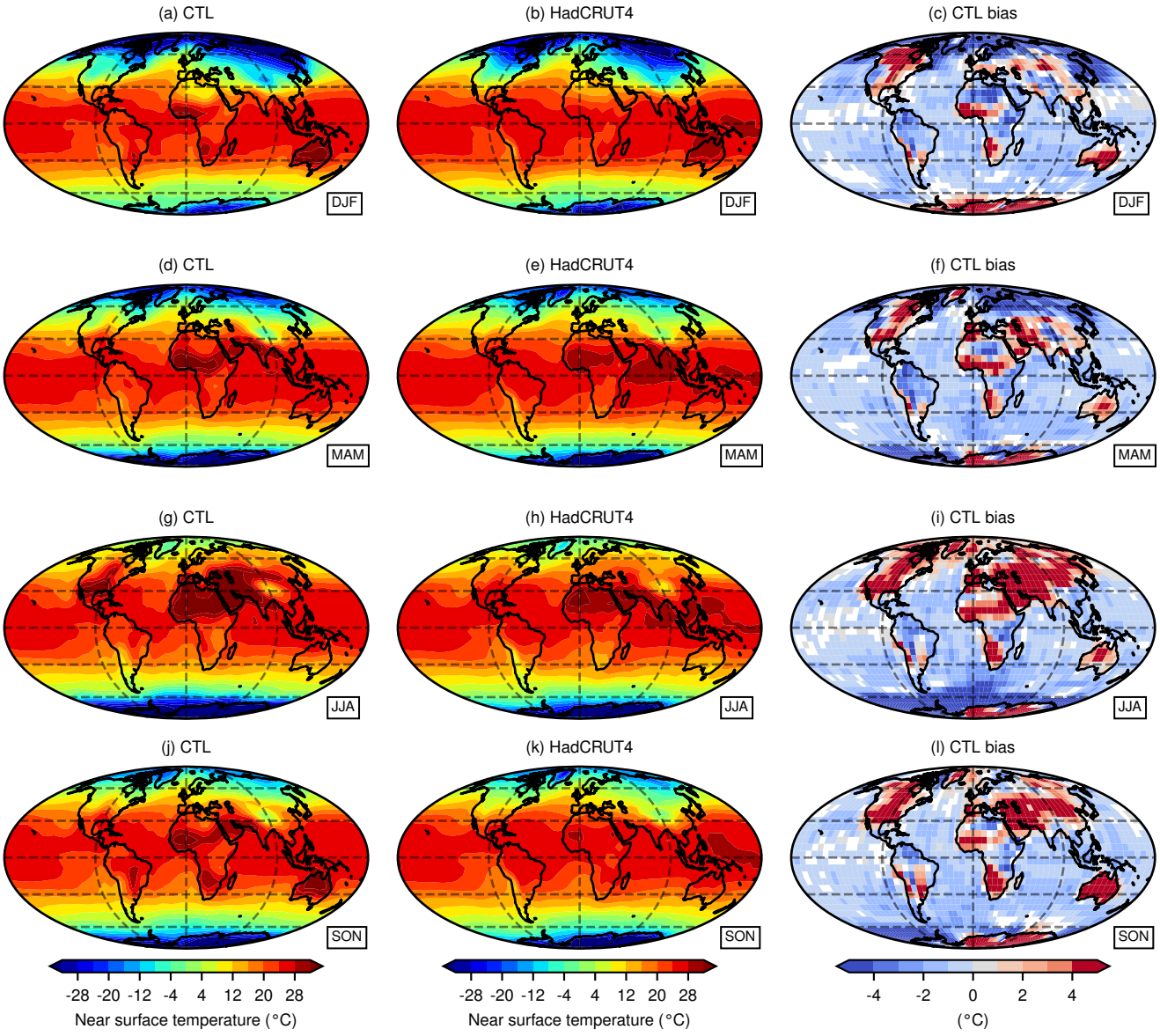

Figure S6. Seasonal means results of near surface temperature for the CTL simulation (a, d, g, j), observational data from HadCRUT4 (b, e, h, k) and model bias (c, f, i, l). In the bias panels, white depicts gridpoints with statistically non-significant difference ($\alpha = 0.05$). Grid lines are spaced every 30° from the Equator and 90° from Greenwich, in latitude and longitude respectively.

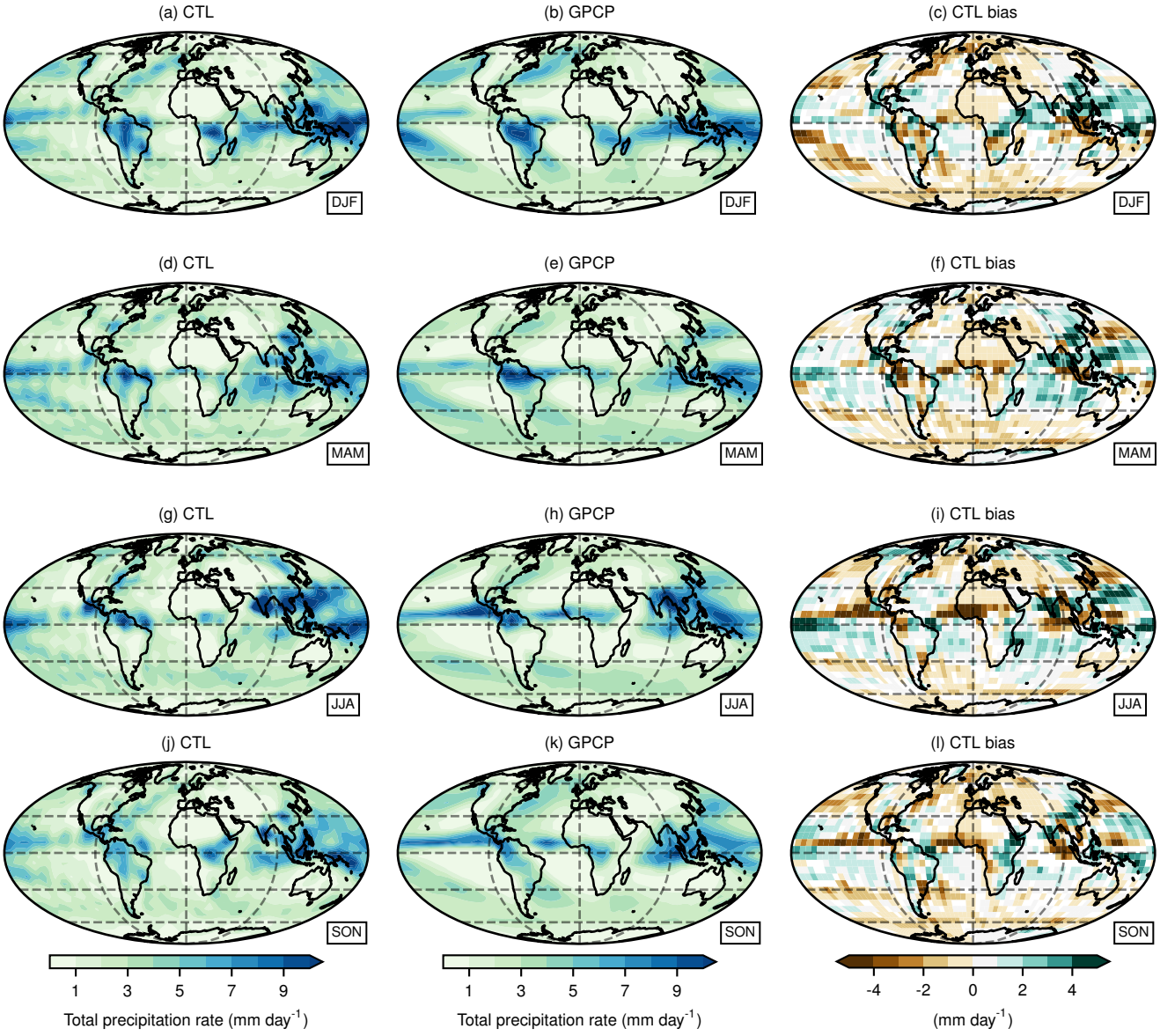

Figure S7. Seasonal means results of total precipitation rate for the CTL simulation (a, d, g, j), observational data from GPCP (b, e, h, k) and model bias (c, f, i, l). In the bias panels, white depicts gridpoints with statistically non-significant difference ($\alpha = 0.05$). Grid lines are spaced every 30° from the Equator and 90° from Greenwich, in latitude and longitude respectively.

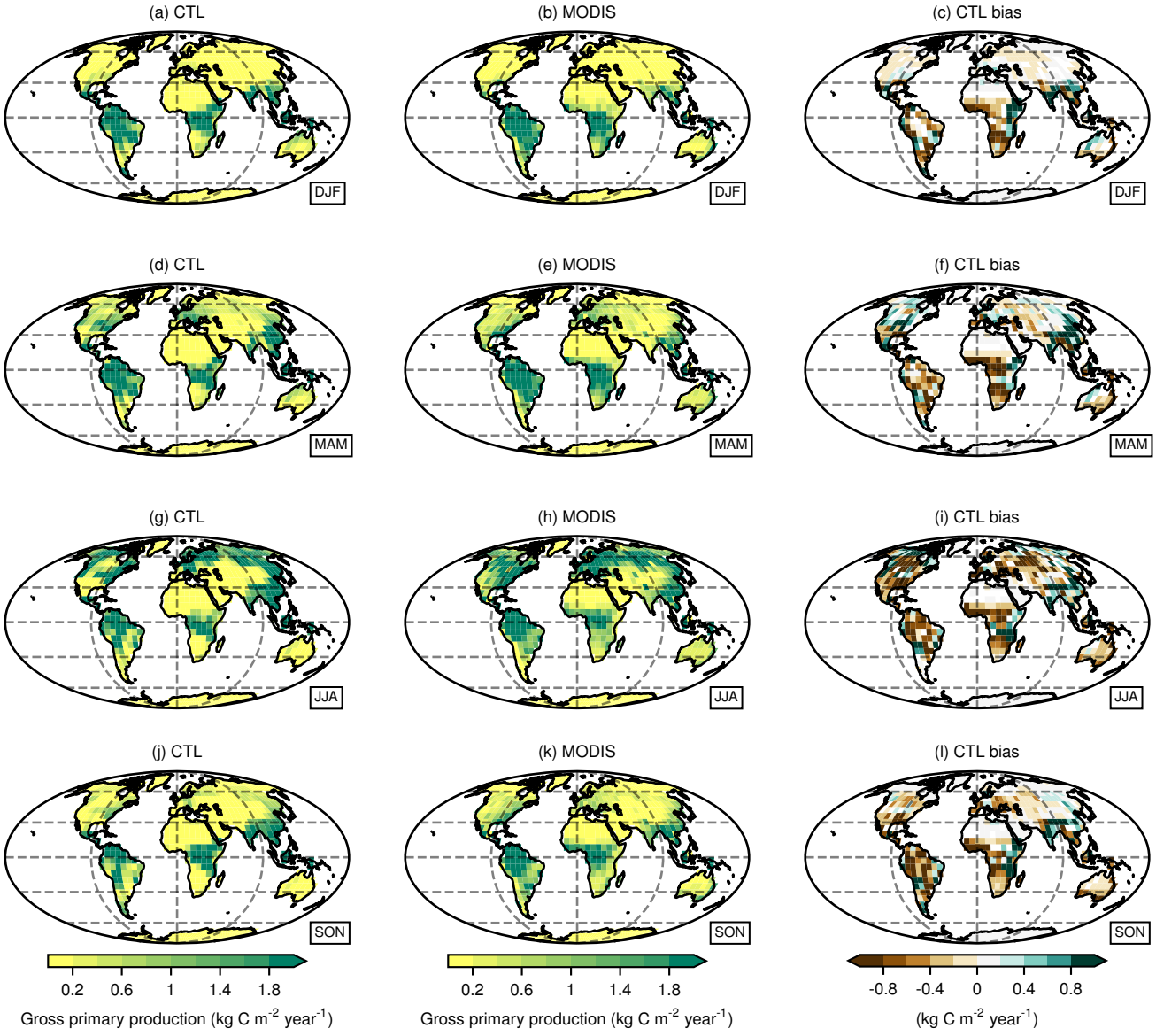

Figure S8. Seasonal means results of GPP for the CTL simulation (a, d, g, j), observational data from MODIS (b, e, h, k) and model bias (c, f, i, l). In the bias panels, white depicts gridpoints with statistically non-significant difference ($\alpha = 0.05$). Grid lines are spaced every 30° from the Equator and 90° from Greenwich, in latitude and longitude respectively.

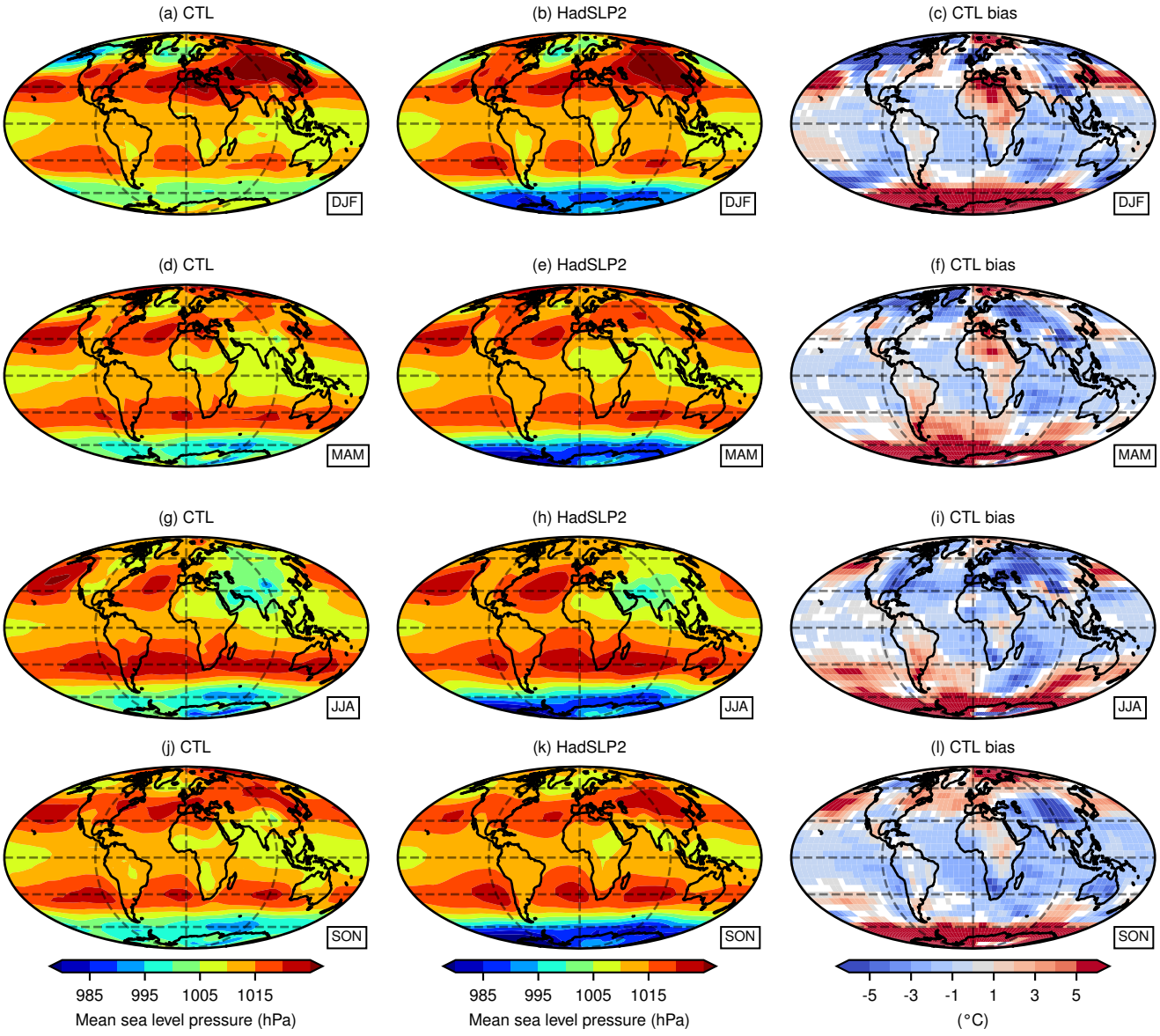

Figure S9. Seasonal means results of mean sea-level pressure for the CTL simulation (a, d, g, j), observational data from HadSLP2 (b, e, h, k) and model bias (c, f, i, l). In the bias panels, white depicts gridpoints with statistically non-significant difference ($\alpha = 0.05$). Grid lines are spaced every 30° from the Equator and 90° from Greenwich, in latitude and longitude respectively.

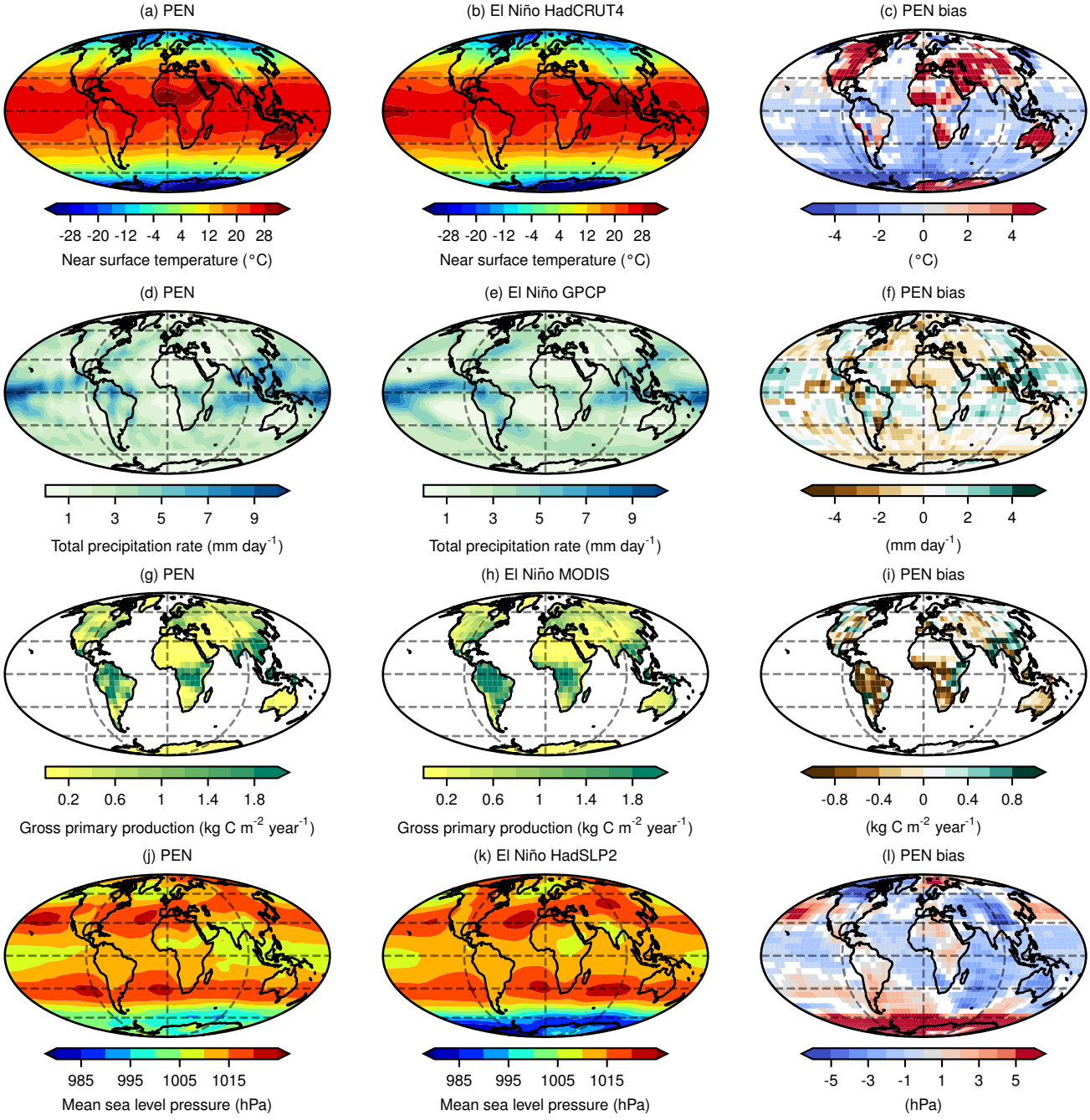

Figure S10. Annual mean results for PEN simulation compared with observational data for El Niño years: near surface temperature in PEN (a), HadCRUT4 mean of 1997–98 and 2015–16 (b), and PEN bias (c); total precipitation rate in PEN (d), GPGP mean of 1997–98 and 2015–16 (e), and PEN bias (f); gross primary production in PEN (g), MODIS mean of 2002–03 and 2009–10 (h) and PEN bias (i); and mean sea-level surface pressure in PEN (j), HadSLP2 mean of 1982–83 and 1997–98 (k), and PEN bias (l). Grid lines are spaced every 30° from the Equator and 90° from Greenwich, in latitude and longitude respectively. In all bias panels white is for statistically non-significant differences ($\alpha = 0.05$).

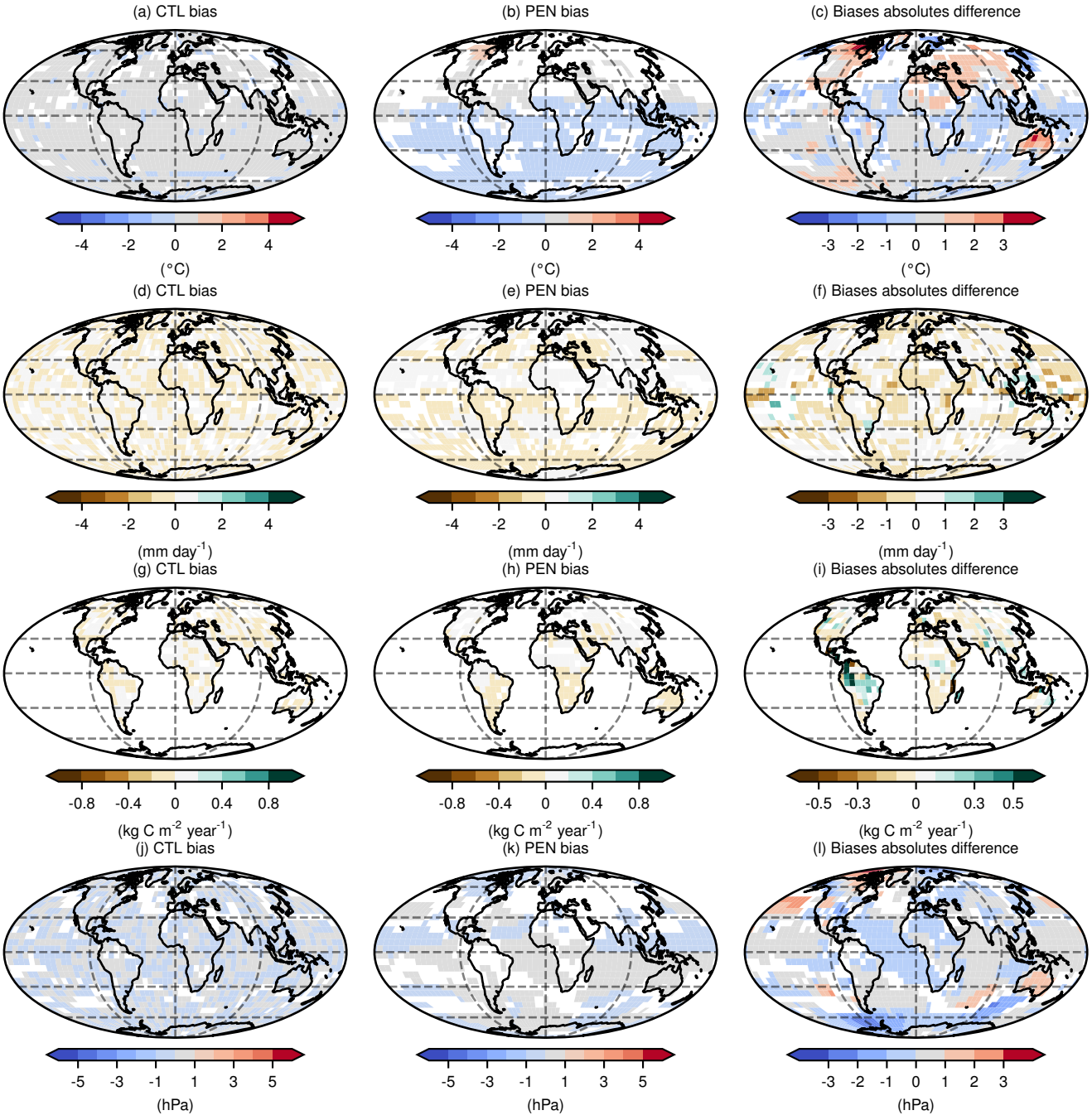

Figure S11. Bias panels from CTL simulation compared with PEN and their absolutes differences for variables: near surface temperature bias in CTL (a), PEN (b) and their differences (c); total precipitation rate bias in CTL (d), PEN (e) and their differences (f); gross primary production bias in CTL (g), PEN (h) and their differences (i); and mean sea-level surface pressure bias in CTL (j), PEN (k) and their differences (l). Grid lines are spaced every 30° from the Equator and 90° from Greenwich, in latitude and longitude respectively. In all panels white is for statistically non-significant differences ($\alpha = 0.05$).

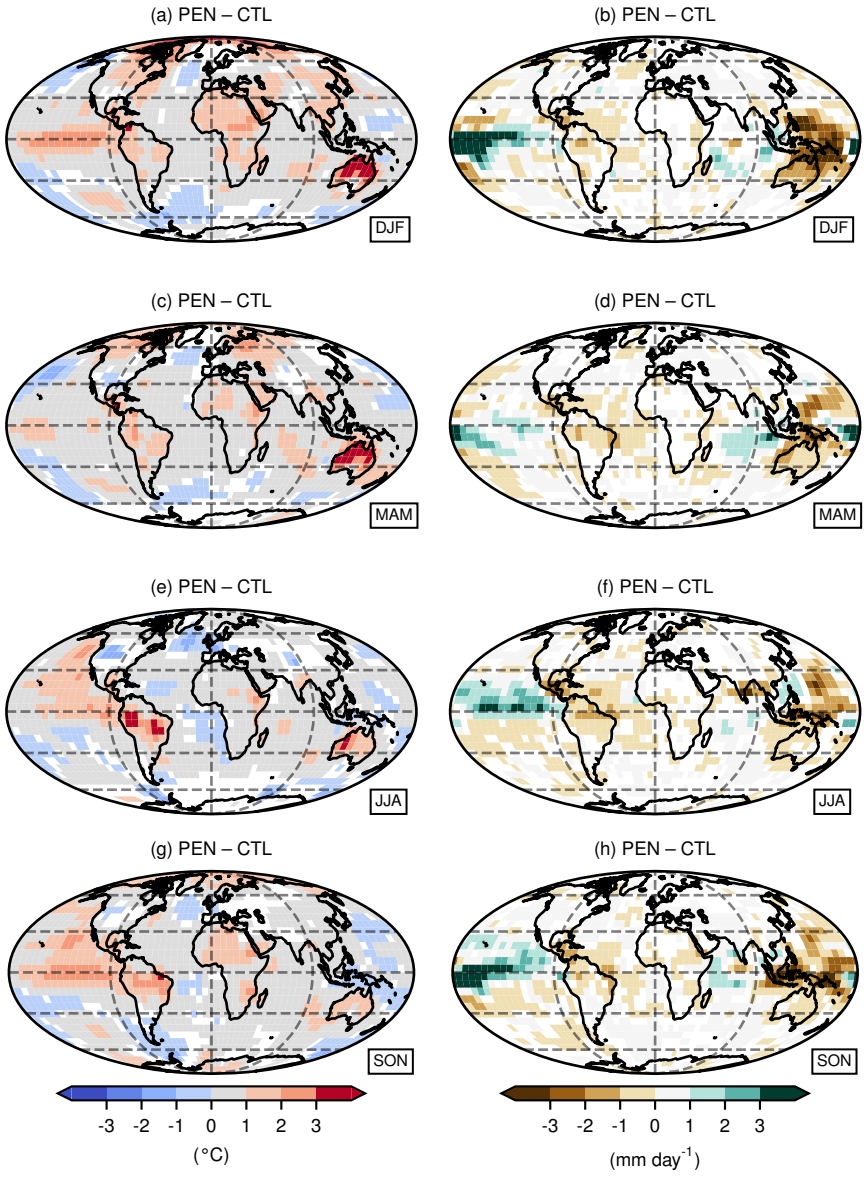

Figure S12. Differences in seasonal means results for the PEN simulation compared with the CTL simulation (PEN minus CTL) of near surface temperature (a, c, e, g) and daily precipitation (b, d, f, h). Grid lines are spaced every 30° from the Equator and 90° from Greenwich, in latitude and longitude respectively. In all panels, white depicts gridpoints with statistically non-significant difference ($\alpha = 0.05$).

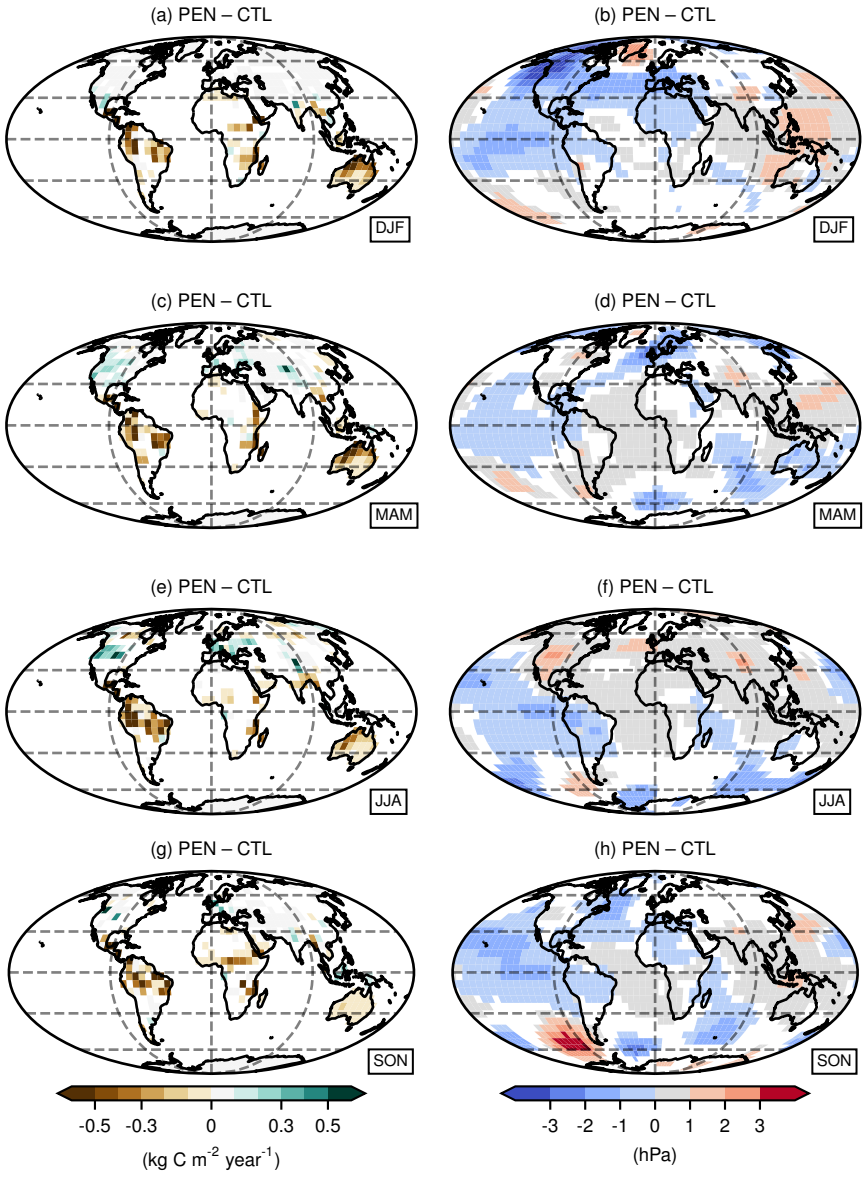

Figure S13. Differences in seasonal means results for the PEN simulation compared with the CTL simulation (PEN minus CTL) of GPP (a, c, e, g) and mean sea-level pressure (b, d, f, h). Grid lines are spaced every 30° from the Equator and 90° from Greenwich, in latitude and longitude respectively. In all panels, white depicts gridpoints with statistically non-significant difference ($\alpha = 0.05$).

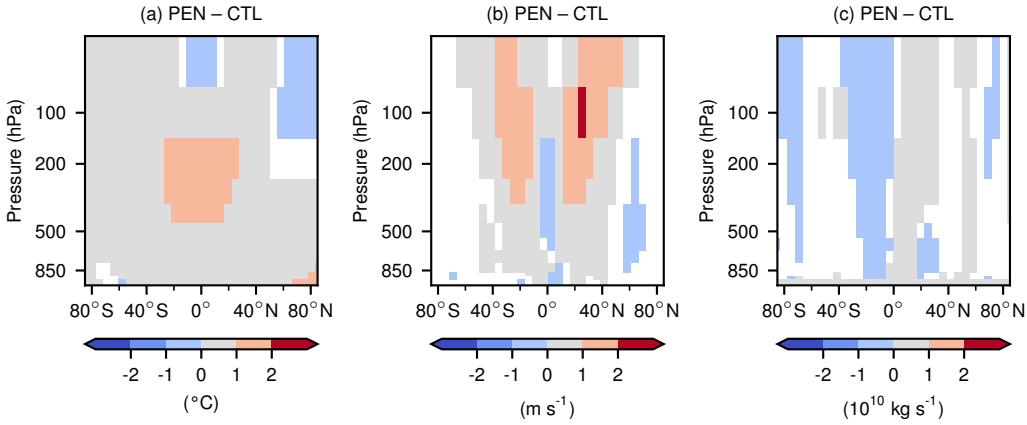

Figure S14. Differences in zonal average annual means for the PEN simulation compared with the CTL simulation (PEN minus CTL) at different pressure levels for: air temperature (a), zonal wind (b) and meridional stream function (c). In all panels, white depicts gridpoints with statistically non-significant difference ($\alpha = 0.05$).

References

Adler, R. F., Huffman, G. J., Chang, A., Ferraro, R., Xie, P.-P., Janowiak, J., Rudolf, B., Schneider, U., Curtis, S., Bolvin, D., et al.: The Version-2 Global Precipitation Climatology Project (GPCP) Monthly Precipitation Analysis (1979-Present), Journal of Hydrometeorology, 4, 1147–1167, https://doi.org/10.1175/1525-7541(2003)004<1147:TVGPCP>2.0.CO;2, 2003.

Allan, R. and Ansell, T.: A New Globally Complete Monthly Historical Gridded Mean Sea Level Pressure Dataset (HadSLP2): 1850-2004, Journal of Climate, 19, 5816–5842, https://doi.org/10.1175/JCLI3937.1, 2006.

Dee, D. P., Uppala, S. M., Simmons, A. J., Berrisford, P., Poli, P., Kobayashi, S., Andrae, U., Balmaseda, M. A., Balsamo, G., Bauer, P., Bechtold, P., Beljaars, A. C. M., van de Berg, L., Bidlot, J., Bormann, N., Delsol, C., Dragani, R., Fuentes, M., Geer, A. J., Haimberger, L., Healy, S. B., Hersbach, H., Hólm, E. V., Isaksen, L., Kållberg, P., Köhler, M., Matricardi, M., McNally, A. P., Monge-Sanz, B. M., Morcrette, J.-J., Park, B.-K., Peubey, C., de Rosnay, P., Tavolato, C., Thépaut, J.-N., and Vitart, F.: The ERA-Interim Reanalysis: Configuration And Performance Of The Data Assimilation System, Quarterly Journal of the Royal Meteorological Society, 137, 553–597, https://doi.org/10.1002/qj.828, 2011.

Dowsett, H., Robinson, M., and Foley, K.: Pliocene three-dimensional global ocean temperature reconstruction, Climate of the Past, 5, 769–783, https://doi.org/10.5194/cp-5-769-2009, 2009.

Hurrell, J. W., Hack, J. J., Shea, D., Caron, J. M., and Rosinski, J.: A New Sea Surface Temperature And Sea Ice Boundary Dataset For The Community Atmosphere Model, Journal of Climate, 21, 5145–5153, https://doi.org/10.1175/2008JCLI2292.1, 2008.

Morice, C. P., Kennedy, J. J., Rayner, N. A., and Jones, P. D.: Quantifying Uncertainties In Global And Regional Temperature Change Using An Ensemble Of Observational Estimates: The HadCRUT4 Data Set, Journal of Geophysical Research: Atmospheres, 117, 1–22, https://doi.org/10.1029/2011jd017187, 2012.

Trenberth, K. E., Fasullo, J. T., and Mackaro, J.: Atmospheric Moisture Transports From Ocean To Land And Global Energy Flows In Reanalyses, Journal of Climate, 24, 4907–4924, https://doi.org/10.1175/2011jcli4171.1, 2011.

Zhao, M., Heinsch, F. A., Nemani, R. R., and Running, S. W.: ImprovementS Of The MODIS Terrestrial Gross And Net Primary Production Global Data Set, Remote Sensing of Environment, 95, 164–176, https://doi.org/10.1016/j.rse.2004.12.011, 2005.